Available online at www.sciencedirect.com
SCIENCE DIRECT®
Journal of Sound and Vibration 290 (2006) 1234–1255
JOURNAL OF SOUND AND VIBRATION
www.elsevier.com/locate/jsvi

Material parameter identification of sandwich beams by an inverse method

Yinming Shi[a,b,*], Hugo Sol[a], Hongxing Hua[b]

[a]*Department of Mechanics of Material and Construction, Vrije Universiteit Brussel, Brussels, Belgium*
[b]*The State Key Lab for Vibration, Shock and Noise, Shanghai Jiao Tong University, Shanghai, China*

Received 5 April 2004; received in revised form 31 March 2005; accepted 16 May 2005
Available online 25 August 2005

Abstract

Sandwich structures are extensively used in engineering because of their high specific stiffness and strength. The modelling of sandwich structures has been studied extensively, but less attention has been paid to their material identification. This paper proposes an inverse method for the material identification of sandwich beams by measured flexural resonance frequencies. The procedure is illustrated with numerically generated test data and also applied on experimentally measured data taken out of literature. An error estimation procedure is conducted to discover and discuss the main error sources.

1. Introduction

Sandwich structures are popular in engineering applications as load-carrying structural members because of their high stiffness and strength-to-weight ratios, good fatigue properties, good thermal and acoustical insulation and ease of mass production [1,2]. The discussion in this paper is limited to sandwich structures, which are defined as three-layer structures consisting of two thin sheets of high-strength material between which a layer of low average strength and

*Corresponding author. Faculty of Applied Science, Department of Mechanics of Material and Construction, Vrije Universiteit Brussel, Pleinlaan 2, B, MEMC, Building KB, 1050 Brussel, Belgium. Tel.: +32 2 629 2983; fax: +32 2 629 2928.
E-mail address: yinming.shi@lmschina.com (Y. Shi).

0022-460X/$ - see front matter © 2005 Elsevier Ltd. All rights reserved.
doi:10.1016/j.jsv.2005.05.026

Nomenclature

A_t, A_b, A_c area of the cross-section of three layers
b the width of sandwich elements
E_t, E_b Young's modulus of the top and bottom face sheet
E_{eq}, G_{eq} the equivalent Young's modulus and equivalent elastic shear modulus of the sandwich beam
E_{BE} the equivalent Young's modulus of the sandwich beam from free–free Euler beam formulas
E_f the Young's modulus of the two identical face sheets ($E_f = E_t = E_b$)
$f_{n\,exp}$ the experimentally measured nth frequency
$f_{i\,exp}, \eta_{i\,exp}$ the ith experimentally measured frequency and loss factor
$f_{i\,cal}, \eta_{i\,cal}$ the ith calculated frequency and loss factor
G_c the elastic shear modulus of the core
h_f the thickness of the two identical face sheet ($h_f = h_t = h_b$)
h_b, h_t, h_c the thickness of the bottom face sheet, top face sheet and the core, respectively
i the node of sandwich beam elements
I_t, I_b moment of inertia of the top and bottom face sheet
j the node of sandwich beam elements
K_{sp} the shape factor (also called the shear correction factor)
L the length of the sandwich beams
L_e length of sandwich elements
$N_w, N_t, N_b, N_{uc}, N_{\gamma c}$ shape function of the transverse displacement of sandwich beam, the axial displacement of the top face sheet, bottom face sheet and the core, the shear strain of the core
t the total thickness of the sandwich beam, $t = h_c + h_t + h_b$
$u_{ti}^{(e)}, u_{tj}^{(e)}$ the axial displacement of top face sheet at node i, j
$u_{bi}^{(e)}, u_{bj}^{(e)}$ the axial displacement of bottom face sheet at node i, j
u_c the axial displacement of the core
U_p potential energy of the sandwich beams
U_k kinetic energy of the sandwich beams
$\{U^{(e)}\}$ local nodal displacement vector
$w_i^{(e)}, w_j^{(e)}$ the transverse displacement of sandwich elements at node i, j
w_n the measured nth circular frequency ($2\pi f_n$) of sandwich beam
w_{nf} the nth circular frequency of the face sheet
x the axial coordinates
ε tolerance in the identification iteration
γ the shear strain of the core
η_n the measured nth modal loss factor of the sandwich beam
η_c the loss factor of the core
$\theta_i^{(e)}, \theta_j^{(e)}$ the rotation of sandwich elements at node i, j
ρ_t, ρ_b, ρ_c density of the cross-section of three layers
ρ the equivalent density of the sandwich beam
ρ_f the density of the two identical face sheets ($\rho_f = \rho_t = \rho_b$)

Superscript

e related to sandwich elements
$'$ partial differentiation with respect to x

Subscript

b related to bottom face sheet
c related to core
e related to sandwich element
f related to the face sheet
i, j related to node i and j
n the nth modal parameters
t related to top face sheet
u related to axial displacement
w related to transverse displacement
γ related to shear strain of the core

density is sandwiched. Depending upon different conditions, the face sheets material can be aluminium alloys [3,4], fibre-reinforced plastics [5–7] or heat-resistant steel [8]. Both the material and geometrical shape of the core can vary widely. Very popular types of core are honeycomb core [3–5], corrugated core [9], foam [6,52], and viscoelastic polymer core [10–13]. Face sheets are typically bounded to the core with an adhesive. They carry most of the bending and in-plane loads. The function of the core is twofold. First, the core keeps the faces separated and stabilizes them. Secondly, the core contributes to the flexural stiffness, out-of-plane shear and compressive strength. The performance of sandwich structures depends mainly on the following factors: (1) the properties of the skin; (2) the core properties; (3) the properties of the used adhesive; (4) the geometrical shape and dimensions of the core.

An important issue in sandwich structures is the knowledge of the values of the material parameters. This is essential for the quality of the model and for eventual static or dynamical analysis. In the appendix of Plantema's book [1], the bending stiffness, shear stiffness, twisting stiffness and Poisson's ratio are determined experimentally by static tests. The Young's modulus, shear modulus and Poisson's ratio could be derived from relatively simple formulas. In Ref. [14], the bending stiffness of a CFRP skin/foam core sandwich beam is evaluated by a three-point bending (TPB) test. A block shear test (BST) procedure is described in ASTM C 273-61 [15], a TPB test procedure is described in ASTM C 273-61 [16]. Both methods are compared in Ref. [17].

All the above methods are based on static testing and can be classified as destructive evaluation methods. A measurement technique for the estimation of the core shear strain in completely enclosed sandwich structures by using delta rosette strain gauge configuration is presented in Ref. [3]. In Ref. [4], aluminium honeycomb sandwich beams are regarded as orthotropic Timoshenko beams. An equivalent Young's modulus and shear modulus are identified from measured flexural resonance frequencies. This can be considered as a non-destructive evaluation (NDE) method, but the material parameters of the face sheets and the core are not considered separately. Wanner and Kromp [18] used five flexural frequencies of beam specimens to identify Young's modulus and the shear modulus based on approximate Timoshenko beam formulas. In 1999, Lins et al. [19] built a new equipment to identify G at up to a temperature of 2000 °C. The methods in Refs. [18,19] are limited to beams with homogeneous cross-section. The ASME standard [20] proposes a procedure to determine material parameters from test beams, but unfortunately, it is only suitable for isotropic material with an assumed relation between Young's modulus, Poisson's ratio and the shear modulus.

Material parameter identification by inverse methods using measured resonance frequencies is a recent type of NDE method. The principle of inverse methods for material identification is to update iteratively the engineering constants in a finite element model of the test specimens in such a way that the computed frequencies match the measured frequencies (see Fig. 1).

The engineering constants that minimize an output residual are considered as the solution of the procedure. The minimization of the output residual is realized by optimization methods, which minimize a scalar value called "the objective function". A typical objective function is the sum of the squared residual components.

The underlying idea of inverse methods based on measurement of resonance frequencies originates from the observation that all constructions made with elastic materials have a characteristic set of resonance frequencies. The values of these frequencies are determined by the geometry, boundary conditions, the elastic moduli and the density of the used materials. Thus,

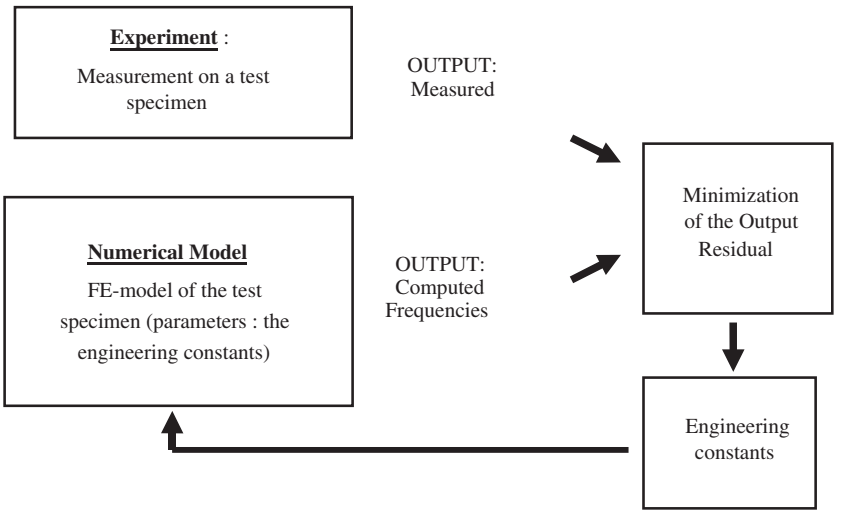

Fig. 1. The principle of an inverse method.

inversely, these resonance frequencies can be used as tools to determine the elastic moduli if the geometry, boundary conditions and the density are assumed to be known.

A lot of research work has been reported in literature about estimation of the material properties of homogeneous beams, plates and simple shells using inverse methods. For thin plates, De Wilde and Sol [21,22], Sol [23] Deobald [24], Deobald and Gibson [25], Frederiksen [26], Moussu and Nivoit [27], and Lai and Ip [28] studied material parameter identification based on Kirchhoff's thin plate theory. For thick plates, in order to include the influence of the transverse shear modulus, Hua [29], Frederiksen [30], Marchand and Authesserre [31], Grédiac and Paris [32], Wang and Kam [33], Shun-Fa Hwang and Chao-Shui Chang [34], Rikards and Chate [35], and Liu et al. [36] investigated material parameter identification based on first-order shear theory (Mindlin plate model) or higher order shear theory. Garne and Martinez [37] studied material parameter identification from the resonance frequencies of shell structures.

In spite of the many applications of sandwich structures, not many researches to identify material properties are conducted based on inverse methods. The goal of this paper is to find a convenient, accurate, simple and NDE minded inverse method to identify material parameters.

The Young's modulus of face sheets and shear modulus of core calculated from formulas based on simple Timoshenko beam theory are used as initial values. The used finite element model is based on sandwich beam theory and the Nelder–Mead (NM) Simplex optimization method is selected as optimization algorithm. Some numerical examples and experiments from literatures are used to illustrate and validate the proposed method. An error estimation is conducted at the end.

2. Material parameter identification by an inverse method

In order to identify material parameters of sandwich beams by an inverse method, several items must be selected: an accurate numerical model, good initial values, a suitable objective function

and a performing optimization programme. The following paragraphs will describe these items one by one in some detail.

2.1. The finite element model

Fig. 2 presents a sandwich beam element. A list of symbols used in the context is given in Nomenclature. The proposed finite element model is developed based on the following assumptions: (1) the shear stresses in the two face sheets and longitudinal normal stresses in the core are negligible; (2) the shear strain is linearized across the depth of the core; (3) the transverse displacement is the same for all the three layers; (4) there is no slipping between the face sheet and the core at their interface; (5) the core is elastic or linearly viscoelastic, with a shear modulus G_c or $G_{c*}(1+\mathrm{i}^*\eta_c)$, where $\mathrm{i}=\sqrt{-1}$. The face sheets are elastic or linearly viscoelastic, with a Young's modulus E_f or $E_{f*}(1+\mathrm{i}^*\eta_f)$, where $\mathrm{i}=\sqrt{-1}$. (6) Density and thickness are uniform over the sandwich beam; (7) the two face sheets are identical.

The sandwich beam finite element model is derived based only on the assumption (1)–(6). For simplicity, assumption (7) is added during the identification process.

The column of nodal displacements becomes:

$$\{U^{(e)}\}=[w_i^{(e)}\ \theta_i^{(e)}\ u_{ti}^{(e)}\ u_{bi}^{(e)}\ w_j^{(e)}\ \theta_j^{(e)}\ u_{tj}^{(e)}\ u_{bj}^{(e)}]^{\mathrm{T}}. \tag{1}$$

The transverse displacement of the sandwich beam and the axial displacements of the two face sheets are expressed in function of the nodal displacements by finite element shape functions:

$$w=[N_w]\{U^{(e)}\},\quad u_t=[N_t]\{U^{(e)}\},\quad u_b=[N_b]\{U^{(e)}\}, \tag{2}$$

where the shape functions are given by

$$[N_w]=\lfloor 1-3\xi^2+2\xi^3\ \ (\xi-2\xi^2+\xi^3)L_e\ \ 0\ \ 0\ \ 3\xi^2-2\xi^3\ \ (-\xi^2+\xi^3)L_e\ \ 0\ \ 0\rfloor,$$

$$[N_t]=[0\ \ 0\ \ 1-\xi\ \ 0\ \ 0\ \ 0\ \ \xi\ \ 0],\quad [N_b]=[0\ \ 0\ \ 0\ \ 1-\xi\ \ 0\ \ 0\ \ 0\ \ \xi].$$

The above expressions use a reduced coordinate: $\xi=x/L_e$.

From the kinematical relationships between the top face sheet and the bottom face sheet, it is easy to derive the following relations [38]:

$$u_c=\frac{u_t+u_b}{2}+\frac{(h_t-h_b)}{4}\frac{\partial w}{\partial x},$$

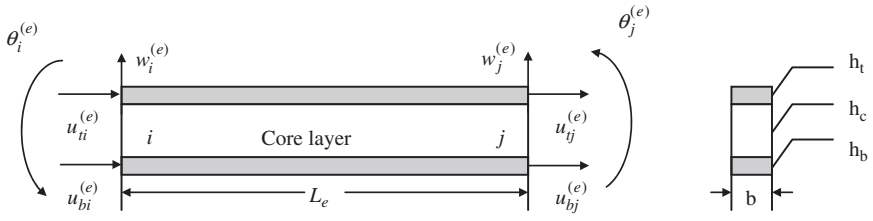

Fig. 2. A sandwich beam element.

$$\gamma = \frac{u_t - u_b}{h_c} + \frac{\partial w}{\partial x}\left(\frac{h_t + h_b + 2h_c}{2h_c}\right). \tag{3}$$

γ and u_c can be expressed in the nodal displacement as follows:

$$u_c = [N_{uc}]\{U^{(e)}\}, \quad \gamma = [N_{\gamma c}]\{U^{(e)}\}, \tag{4}$$

where

$$[N_{uc}] = \frac{1}{2}([N_t] + [N_b]) + \frac{h_t - h_b}{4}[N_w]',$$

$$[N_{\gamma c}] = \frac{1}{h_c}\left[-\frac{6h^*}{L_e}\xi + \frac{6h^*}{L_e}\xi^2 \;\; h^*(1 - 4\xi + 3\xi^2) \;\; 1 - \xi \;\; \xi - 1 \;\; \frac{6h^*}{L_e}\xi - \frac{6h^*}{L_e}\xi^2 \;\; h^*(-2\xi + 3\xi^2) \;\; \xi - \xi\right],$$

$$h^* = (h_t - h_b)/4.$$

The potential energy and the kinetic energy of the sandwich beam can be written as follows:

$$U_p = \frac{1}{2}E_tA_t\int_0^{L_e}(u_t')^2\,\mathrm{d}x + \frac{1}{2}E_bA_b\int_0^{L_e}(u_b')^2\,\mathrm{d}x + \frac{1}{2}K_{sp}G_cA_c\int_0^{L_e}\gamma^2\,\mathrm{d}x + \frac{1}{2}(E_tI_t + E_bI_b)\int_0^{L_e}(w'')^2\,\mathrm{d}x, \tag{5}$$

$$U_k = \frac{1}{2}\rho_tA_t\int_0^{L_e}\dot{u}_t^2\,\mathrm{d}x + \frac{1}{2}\rho_bA_b\int_0^{L_e}\dot{u}_b^2\,\mathrm{d}x + \frac{1}{2}\rho_cA_c\int_0^{L_e}\dot{u}_c^2\,\mathrm{d}x + \frac{1}{2}(\rho_tA_t + \rho_bA_b + \rho_cA_c)\int_0^{L_e}\dot{w}^2\,\mathrm{d}x. \tag{6}$$

In the above equation (5), the shape factor K_{sp} is also called the shear correction factor. In most papers about sandwich beams such as Refs. [39,40], K_{sp} is ignored without adequate explanation. In Ref. [41], K_{sp} is introduced, but the origin of the used value of K_{sp} in the text is not clear. In Ref. [42], six different methods of evaluation for K_{sp} are compared. Unlike the common used value of $K_{sp} = 5/6$ for homogeneous cross-section, $K_{sp} = 1$ is recommended in Ref. [42] for sandwich beams. Hence the recommended $K_{sp} = 1$ is used in Eq. (5).

The free vibration equation of the sandwich element can be derived by using the principles of virtual work. The dynamic equation of the whole sandwich beam can be obtained through standard finite element assembling procedures.

2.2. Initial values

In inverse methods, good initial values can limit the necessary number of iteration cycles. This not only saves computer time during the identification process, but it also avoids evolving into a local minimum instead of the desired global minimum. By using assumption (7) in Section 2.1 ($E_f = E_t = E_b$), initial values for the material properties in sandwich beams with a free–free boundary condition can be obtained through three steps.

Step 1: the sandwich beam is regarded as a Timoshenko Beam. The equivalent Yong's modulus E_{eq} and equivalent shear modulus G_{eq} can be calculated from the resonance frequencies by using the following formulas [18]:

$$E_{eq} = A_n + B_n * \frac{E_{eq}}{G_{eq}} \tag{7.1}$$

with

$$A_n = E_{BE}\left(1 + a_n \frac{t^2}{L^2}\right), \tag{7.2}$$

$$B_n = E_{BE}\left(b_n \frac{t^2}{L^2} - c_n \frac{t^4}{L^4}\right), \tag{7.3}$$

$$E_{BE} = \frac{48\rho\pi^2 L^4}{t^2 m_n^4} f_{n\,exp}^2. \tag{7.4}$$

Table 1 lists the constants in the above formulas for the sixth first flexural mode shape numbers.

Formula (7) is used to obtain Young's modulus E_{eq} and the transverse shear modulus G_{eq}. Formula (7) must be evaluated for at least two different sets of values.

Step 2: the Young's modulus E_f of the two identical face sheets and the elastic shear modulus G_c of the core can be calculated approximately from the obtained equivalent Young's modulus E_{eq} and equivalent shear modulus G_{eq} by the following formulas [3]:

$$(EI)_{eq} = \frac{E_f b h_f^3}{6} + \frac{E_f b h_f (h_c + h_f)^2}{2}, \tag{8.1}$$

$$(GA)_{eq} = G_c * b * h_c. \tag{8.2}$$

$(EI)_{eq}$ is the equivalent bending stiffness, $(AG)_{eq}$ is the equivalent shear stiffness. Both can easily be calculated from the equivalent Young's modulus E_{eq} and equivalent shear modulus G_{eq} obtained from (7). Formula (8) is more suitable for sandwich beams with relatively thin, stiff face sheets and relatively soft, thick core.

Table 1
Constants of free–free Timoshenko beam formulas

Mode No. n	m_n	a_n	b_n	c_n
1	4.7300	4.12	1.23	4.20
2	7.8532	9.08	4.60	32.0
3	10.996	15.6	9.89	122
4	14.137	23.7	17.2	333
5	17.279	33.5	26.4	746
6	20.420	45.0	37.6	1449

Step 3: In sandwich structures, the damping property is usually an important parameter. There are several definitions of damping. Among them, the specific damping capacity ψ, expressed as the ratio of energy dissipation per loading cycle to the maximum storage energy during the cycle; the logarithmic decrement δ measured in free vibration decay experiment; the modal loss factor η_{mod}, determined by the half-power bandwidth method or 3 dB method; the material loss factor η_{mat}, defined as the ratio of the imaginary to the real part of the material complex modulus. For low levels of damping ($\eta_{\mathrm{mod}} < 0.2$), their inter relationship is given by

$$\psi = 2\delta = 2\pi\eta_{\mathrm{mod}} = 2\pi\eta_{\mathrm{mat}} = 2\pi\frac{\Delta\omega_{3\,\mathrm{dB}}}{\omega_n} = 2\pi\ \tan\ \phi,$$

where ϕ is the phase angle between cyclic stress and strain, ω_n is the resonance peak value, $\Delta\omega_{3\,\mathrm{dB}}$ is determined from the half-power point down from the resonant peak value [43].

If it is required to identify the material loss factor η_c of the core, a simplified Ross–Kervin–Ungar (RKU) equation [8] can be used to estimate its initial value according to the

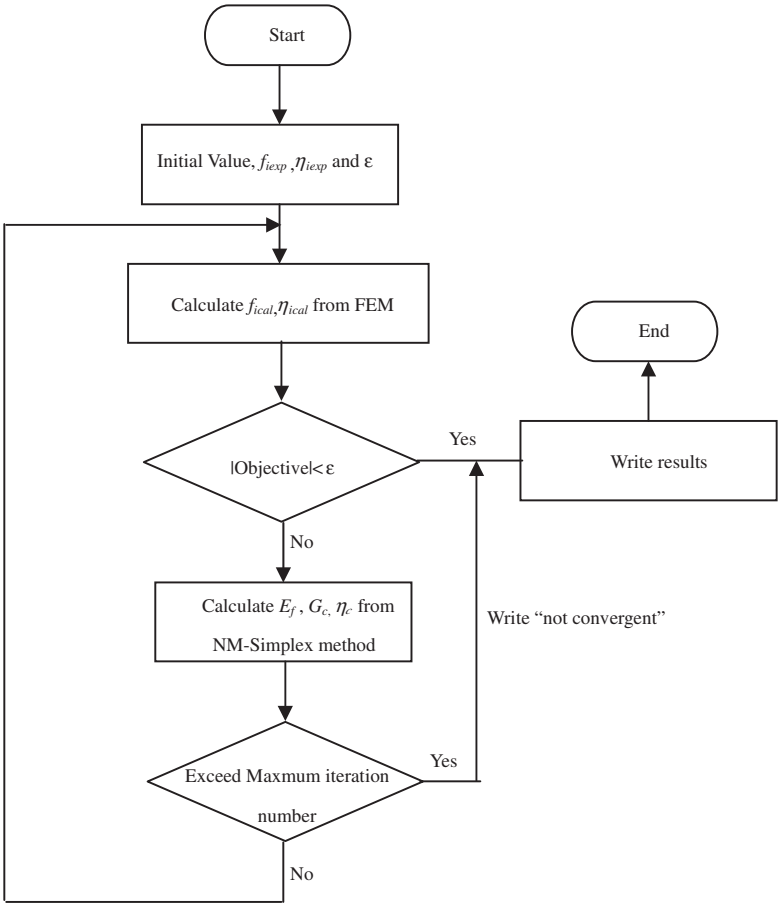

Fig. 3. Flowchart of the whole identification process.

following formulas:

$$\eta_c = \frac{A\eta_n}{A - B - 2(A - B)^2 - 2(A\eta_n)^2}, \tag{9}$$

where

$$A = \left(\frac{w_n}{w_{nf}}\right)^2 \left(2 + \frac{\rho_c}{\rho_f}.\frac{h_c}{h_f}\right)\left(\frac{B}{2}\right), \quad B = \frac{1}{6(1 + h_c/h_f)^2}.$$

w_n is the measured nth circular frequency of sandwich beam. w_{nf} is the nth circular frequency of the face sheet. Since the Young's modulus E_f of the two identical face sheets has already identified from Eq. (8) in Step 2, for a free–free boundary condition, w_{nf} can be easily estimated from an equation similar to Eq. (7.4). η_n is the nth modal loss factor determined by half-power bandwidth method or 3 dB method.

2.3. The optimization process

Optimization methods can minimize the output residual in an inverse method by the selection of an adequate scalar objective function that contains the residual as a variable. The objective function selected in this paper can be written as

$$\text{Objective function} = \sum_{i=1}^{N} \left(1 - \frac{f_{i\text{cal}}}{f_{i\,\text{exp}}}\right)^2 \tag{10}$$

for sandwich beams without considering the loss factor η_c.

$$\text{Objective function} = \sum_{i=1}^{N} \left(1 - \frac{f_{i\text{cal}}}{f_{i\,\text{exp}}}\right)^2 + \sum_{i=1}^{N} \left(1 - \frac{\eta_{i\text{cal}}}{\eta_{i\,\text{exp}}}\right)^2 \tag{11}$$

for sandwich beams including the loss factor η_c.

A direct search method called the NM simplex (NM SPX) optimization method [44] is selected in this paper. The flowchart of the whole identification process is shown in Fig. 3.

3. Error estimation

Consider a numerical model of a test specimen with a relationship between n frequencies, r target parameters (such as Young's moduli, shear moduli) and s test specimen parameters (such as lengths, thicknesses, widths and masses). At given target and test specimen parameter values, finite uncertainty intervals of frequency values due to finite target and test specimen uncertainty

intervals can be approximated as

$$\begin{Bmatrix} \Delta f_1 \\ \Delta f_2 \\ \vdots \\ \Delta f_n \end{Bmatrix} = \begin{bmatrix} \frac{\partial f_1}{\partial p_1} & \frac{\partial f_1}{\partial p_2} & \cdots & \frac{\partial f_1}{\partial p_r} & \frac{\partial f_1}{\partial g_1} & \frac{\partial f_1}{\partial g_2} & \cdots & \frac{\partial f_1}{\partial g_s} \\ \frac{\partial f_2}{\partial p_1} & \frac{\partial f_2}{\partial p_2} & \cdots & \frac{\partial f_2}{\partial p_r} & \frac{\partial f_2}{\partial g_1} & \frac{\partial f_2}{\partial g_2} & \cdots & \frac{\partial f_2}{\partial g_s} \\ \vdots & \vdots & \cdots & \vdots & \vdots & \vdots & \cdots & \vdots \\ \frac{\partial f_n}{\partial p_1} & \frac{\partial f_n}{\partial p_2} & \cdots & \frac{\partial f_n}{\partial p_r} & \frac{\partial f_n}{\partial g_1} & \frac{\partial f_n}{\partial g_2} & \cdots & \frac{\partial f_n}{\partial g_s} \end{bmatrix} \begin{Bmatrix} \Delta p_1 \\ \Delta p_2 \\ \vdots \\ \Delta p_r \\ \Delta g_1 \\ \Delta g_2 \\ \vdots \\ \Delta g_s \end{Bmatrix}. \tag{12}$$

The input parameters for the inverse method are the n frequencies and s test specimen parameters. The relative uncertainties Δp on the r target parameters due to the uncertainties on the $n+s$ input parameters can be computed as [45,46]

$$\Delta p = \begin{bmatrix} s_p^+ & -s_p^+ . s_g \end{bmatrix} \begin{Bmatrix} \Delta f \\ \Delta g \end{Bmatrix}, \tag{13}$$

where

$$s_p^+ \text{ is the pseudo-inverse of } s_p$$

and

$$s_p = \begin{bmatrix} \frac{\partial f_1}{\partial p_1} & \frac{\partial f_1}{\partial p_2} & \cdots & \frac{\partial f_1}{\partial p_r} \\ \frac{\partial f_2}{\partial p_1} & \frac{\partial f_2}{\partial p_2} & \cdots & \frac{\partial f_2}{\partial p_r} \\ \vdots & \vdots & \vdots & \vdots \\ \frac{\partial f_n}{\partial p_1} & \frac{\partial f_n}{\partial p_2} & \cdots & \frac{\partial f_n}{\partial p_r} \end{bmatrix}, \quad s_g = \begin{bmatrix} \frac{\partial f_1}{\partial g_1} & \frac{\partial f_1}{\partial g_2} & \cdots & \frac{\partial f_1}{\partial g_s} \\ \frac{\partial f_2}{\partial g_1} & \frac{\partial f_2}{\partial g_2} & \cdots & \frac{\partial f_2}{\partial g_s} \\ \vdots & \vdots & \vdots & \vdots \\ \frac{\partial f_n}{\partial g_1} & \frac{\partial f_n}{\partial g_2} & \cdots & \frac{\partial f_n}{\partial g_s} \end{bmatrix}. \tag{14}$$

The uncertainty intervals of the input parameters can be stored in a global column $\{\Delta m\} = \begin{Bmatrix} \Delta f \\ \Delta g \end{Bmatrix}$.

The relative contribution of the uncertainty of the jth input parameter on the uncertainty of the ith identified material parameter can be computed [46–48]:

$$\rho_i = \frac{|s_{ij}| . \Delta m_j}{\sum_{j=1}^{n+s} |s_{ij}| . \Delta m_j}, \quad i = 1, 2, \ldots, r \tag{15}$$

with

$$[s] = \begin{bmatrix} s_p^+ & -s_p^+ . s_g \end{bmatrix}. \tag{16}$$

Relation (15) satisfies the consistency condition [45]:

$$\sum_{j=1}^{n+s} \rho_{ij} = 1, \quad i = 1, 2, \ldots, r. \tag{17}$$

4. Case studies

An accurate mathematic model is a prerequisite of material parameters identification by inverse methods. This section therefore will compare first the finite element model of the sandwich beams built in Section 2 with models from literature. Three different test cases will be presented. Next, the identification procedure results will be verified with experimental results and numerical simulations. Finally, an error estimation example will be given.

4.1. Verification of the sandwich finite element model

Test case 1: In this test case, the damping of neither face sheets nor the core layer is considered.

A sandwich beam with face sheets made from glass fibre reinforced plastics (GFRP) and a core layer made from PVC is studied in detail in Ref. [6]. The resonance frequencies are derived from wave propagation equations. The results from the proposed sandwich finite element model are compared with those from wave propagation model. The properties of the sandwich beam are listed in Table 2. The boundary condition is free–free. The calculated resonance frequencies both from Ref. [6] and from current study, the measured frequencies, and the corresponding relative errors are listed in Table 3.

From Table 3, the following conclusion can be drawn: (1) by comparing the current results with those calculated in Ref. [6] (see the fifth column in Table 3), it is clear that both the current sandwich finite element model and the wave propagation model are very close to each other; (2) by comparing the calculated results with experimental results in Ref. [6] (see the sixth column in Table 3), it can be seen that the results both from the current calculation and from the calculation in Ref. [6] have a non-neglectable difference as compared with the experimental results. This discrepancy results from the inaccurate input material properties in Table 2. In Ref. [6], the E modulus of the GFRP face sheet and G modulus of the PVC core are measured as follows:

(1) First, the GFRP face sheet is measured separately. The face sheet is suspended by using very soft cord to simulate the free–free boundary condition. The E modulus is calculated from the measured frequencies using Euler's formula of a free–free beam vibration.

Table 2
Properties of sandwich beam

	Density (kg/m^3)	E modulus (Pa)	Thickness (m)	Length (m)	Width (m)	Poisson's ratio
GFRP	1580	9.80e9	2.5e-3	1.65	116e-3	0.3
PVC	101	9.40e7	50e-3	1.65	116e-3	0.3

Table 3
Resonance frequencies comparison

Frequency No.	Current model (Hz)	Results in Ref. [6] (Hz)	Measured (Hz)	Relative error with Ref. [6] (%)	Relative error with measurement in Ref. [6] (%)
1	64.189	65	62	−1.247	3.531
2	161.532	162	161	−0.289	0.330
3	282.588	283	288	−0.145	−1.879
4	413.240	412	428	0.301	−3.449
5	546.822	545	578	0.334	−5.394

(2) Secondly, a beam made with only the PVC core is measured separately. The resonance frequencies are measured similarly as in (1). The E modulus is calculated again from the resonance frequencies using Euler's formula. By using the formula of isotropic material ($G = E/2(1+\mu)$) and assuming a value of Poisson's ratio equal to 0.3, the shear modulus G is calculated.

It is clear that the input E modulus of the GFRP face sheets and the G modulus of the PVC core are inaccurate. Several influence factors are missing during the course of deriving the E modulus and the G modulus: (1) for the thick, soft PVC core, Euler's beam free–free vibration formula is not accurate because of the influence of the transverse shear modulus (2). The material properties of the face sheets and the core are different before and after their assemblage into the sandwich beam. The influence of the adhesive layer between the face sheets and the core in sandwich beams cannot be ignored. This is exactly the reason why a more accurate, convenient way is needed to identify the material properties of the sandwich beam instead of measuring them separately (3). The shear modulus of the core is calculated from an assumed Poisson's ratio of 0.3. This results in an inaccurate shear modulus.

Test case 2: In this test case, only the damping of the core is considered. The test case is used to show that the results from different models taken from literature are comparable with the proposed finite element model.

The second case has been extensively studied in various analyses and experiments by several different researchers using different methods. Kerven first studied infinite length beam by using an effective stiffness method and the classical fourth-order theory of elastic beams in Ref. [49]. Mead and Markus [50] derived a sixth-order theory for finite length beam. This problem was also studied by Johnson, Kienholz and Rogers (JKR) [51] with finite element method and modal strain energy (MSE) method. Recently Macé [39] studied this problem by his proposed finite element method and Fasana and Marchesiello [40] analysed it by Rayleigh–Ritz method.

The material properties of the studied cantilever beam are listed in Table 4. The calculated frequencies and modal loss factors are listed in Tables 5–10.

It can be seen that the results from the proposed method can predict the resonance frequencies and modal loss factors and that the results are in good agreement with those from literature.

Test case 3: In this case, the damping of both the face sheets and the core are considered.

Table 4
The material properties of the studied cantilever sandwich beam

	Thickness (m)	Length (m)	Width (m)	Density (Kg/m^3)	E (Pa)	G (Pa)	Poisson's ratio	Loss factor
Face sheet	1.52e-3	0.1778	1.27e-2	2.8e3	6.9e10	—	0.3	0
Core	0.127e-3	0.1778	1.27e-2	968.3	—	0.69e6	—	0.1, 0.2, 0.3, 0.6, 1.0, 1.5

Table 5
Results comparison of the cantilever sandwich beam with core loss factor 0.1

Mode number			1	2	3	4	5
	Mead and Markus	f_n (Hz)	64.075	296.41	743.7	1393.9	2261.09
	[50]	η_n (%)	2.815	2.424	1.54	0.889	0.573
	JKR	f_n (Hz)	64.2	297.0	747.2	1408.3	2304.0
	[51]	η_n (%)	2.817	2.425	1.534	0.878	0.559
$\eta_c = 0.1$	Macé	f_n (Hz)	60.9	288.8	732.9	1381.4	2246.6
	[39]	η_n (%)	2.646	2.173	1.328	0.742	0.463
	Fasana and Marchesiello	f_n (Hz)	63.35	292.1	732.8	1373	—
	[40]	η_n (%)	2.86	2.43	1.54	0.89	—
	Proposed	f_n (Hz)	63.61	294.20	738.02	1383.06	2243.21
	model	η_n (%)	2.81	2.43	1.54	0.89	0.574

Table 6
Results comparison of the cantilever sandwich beam with core loss factor 0.2

Mode number			1	2	3	4	5
	Mead and Markus	f_n (Hz)	64.21	296.64	743.85	1394.0	2261.15
	[50]	η_n (%)	5.56	4.83	3.08	1.776	1.144
	JKR	f_n (Hz)	64.4	297.6	748.0	1409.0	2304.0
	[51]	η_n (%)	5.564	4.832	3.066	1.756	1.118
$\eta_c = 0.2$	Macé	f_n (Hz)	61.2	289.0	733.4	1381.7	2246.9
	[39]	η_n (%)	5.292	4.346	2.656	1.484	0.926
	Fasana and Marchesiello	f_n (Hz)	—	—	—	—	—
	[40]	η_n (%)	—	—	—	—	—
	Proposed	f_n (Hz)	63.74	294.43	738.18	1383.14	2243.27
	model	η_n (%)	5.56	4.83	3.09	1.78	1.14

The third case was studied by both Macé [39] and Fasana and Marchesiello [40]. It is a free–free sandwich beam with GFRP face sheets and a core made of vibrachoc VIB12 at 20 °C. The material properties are listed in Table 11. In this case, the loss factor of both the GFRP face sheet and core is included.

The calculated modal frequencies and modal loss factors are listed in Table 12.

Table 7
Results comparison of the cantilever sandwich beam with core loss factor 0.3

Mode number			1	2	3	4	5
	Mead and Markus	f_n (Hz)	64.43	297.01	744.1	1394.0	2261.24
	[50]	η_n (%)	8.169	7.197	4.614	2.664	1.716
	JKR	f_n (Hz)	64.7	298.0	748.2	1409.5	2305.0
	[51]	η_n (%)	8.175	7.203	4.593	2.634	1.68
$\eta_c = 0.3$	Macé	f_n (Hz)	61.5	289.8	734.0	1382.3	2247.2
	[39]	η_n (%)	7.938	6.519	3.984	2.226	1.389
	Fasana and Marchesiello	f_n (Hz)	—	—	—	—	—
	[40]	η_n (%)	—	—	—	—	—
	Proposed	f_n (Hz)	63.957	294.796	738.432	1383.283	2243.357
	model	η_n (%)	8.165	7.204	4.622	2.670	1.720

Table 8
Results comparison of the cantilever sandwich beam with core loss factor 0.6

Mode number			1	2	3	4	5
	Mead and Markus	f_n (Hz)	65.48	298.9	745.48	1394.9	2261.7
	[50]	η_n (%)	14.76	13.938	9.168	5.316	3.432
	JKR	f_n (Hz)	65.5	301.0	753.0	1414.0	2310.0
	[51]	η_n (%)	14.772	13.956	9.126	5.256	3.36
$\eta_c = 0.6$	Macé	f_n (Hz)	62.7	292.4	737.4	1385.2	2249.7
	[39]	η_n (%)	15.876	13.038	7.968	4.452	2.778
	Fasana and Marchesiello	f_n (Hz)	—	—	—	—	—
	[40]	η_n (%)	—	—	—	—	—
	Proposed	f_n (Hz)	65.005	296.675	739.793	1384.016	2243.847
	model	η_n (%)	14.750	13.949	9.178	5.326	3.437

Table 9
Results comparison of the cantilever sandwich beam with core loss factor 1.0

Mode number			1	2	3	4	5
	Mead and Markus	f_n (Hz)	67.41	302.8	748.6	1396.6	2262.88
	[50]	η_n (%)	20.22	21.77	15.02	8.81	5.7
	JKR	f_n (Hz)	67.4	307.0	762.0	1422.0	2316.0
	[51]	η_n (%)	20.19	21.8	15	8.73	5.6
$\eta_c = 1.0$	Macé	f_n (Hz)	64.3	296.7	744.3	1391.0	2254.8
	[39]	η_n (%)	26.46	21.72	13.28	7.42	4.63
	Fasana and Marchesiello	f_n (Hz)	—	—	—	—	—
	[40]	η_n (%)	—	—	—	—	—
	Proposed	f_n (Hz)	66.913	300.533	742.92	1385.684	2244.98
	model	η_n (%)	20.202	21.72	15.023	8.828	5.714

Table 10
Results comparison of the cantilever sandwich beam with core loss factor 1.5

Mode number			1	2	3	4	5
$\eta_c = 1.5$	Mead and Markus [50]	f_n (Hz)	69.88	308.85	754.0	1399.7	2265.0
		η_n (%)	22.956	29.625	21.9	13.095	8.52
	JKR [51]	f_n (Hz)	70.0	315.0	774.0	1433.0	2328.0
		η_n (%)	22.83	29.28	21.855	13.02	8.385
	Macé [39]	f_n (Hz)	64.4	303.5	755.3	1400.6	2263.8
		η_c (%)	26.46	32.58	19.92	10.86	6.945
	Fasana and Marchesiello [40]	f_n (Hz)	69.13	304.3	743.4	1378	—
		η_n (%)	23.4	29.6	21.9	13.1	—
	Proposed model	f_n (Hz)	69.366	306.555	748.725	1388.773	2247.120
		η_n (%)	22.938	29.651	21.931	13.122	8.534

Table 11
The material properties of the free–free sandwich beam

	Length (m)	Width (m)	Thickness (m)	Density (Kg/m^3)	E (Pa)	G (Pa)	Loss factor
GFRP	0.6	3e-2	10.2e-3	1890	2.4e10	—	0.005
VIB12 Core	0.6	3e-2	1e-3	1100	—	2.2e7	0.73

Table 12
Modal parameters of a free–free sandwich beam

	1		2		3	
	f_1 (Hz)	η_1 (%)	f_2 (Hz)	η_2 (%)	f_3 (Hz)	η_3 (%)
RKU [8] approximation	—	12	—	19	—	22
Macé [39]	193	8.8	493	17.5	900	22.3
Macé experiments [39]	202	8.9	512	18	941	24.7
Fasana and Marchesiello [40]	205	7.4	516	15.7	938	20.8
Proposed	209.51	6.19	516.73	15.76	897.05	21.49

From the above table, it can be seen that the results from the proposed sandwich finite element model are in good agreement with results from literature. The discrepancy with the experimental values results probably from inaccurate input of material parameters, especially for the shear modulus and loss factor of the core.

4.2. *Verification of the material parameters identification procedure*

In this paragraph, the material parameters identification procedure is verified by experiments and numerical examples.

Test case 1: The sandwich beam with GFRP face sheets and PVC core studied in case 1 in Section 4.1 is used to validate the material parameters (Elastic Young's modulus of face sheets E_f and elastic shear modulus G_c) identification from the experimental measured first five resonance frequencies by the proposed procedure in Section 2.

The proposed sandwich model used the geometrical parameters and densities in Table 2 and the measured first five frequencies in Table 3. Next, according to steps 1 and 2 in Section 2.2, the initial values and the identified values are computed. The results together with the values from Ref. [6] are listed in Table 13.

The measured first 10 frequencies (taken from Ref. [6]) are compared with predicted frequencies using the final identified parameters and the values from Ref. [6] in the proposed finite element model. The results and their relative errors are listed in Table 14.

From the above results, the following conclusion can be drawn: (1) comparing the relative errors in columns 3 (relative errors between columns 1 and 2) and 5 (relative errors between columns 1 and 4), it is clear that the frequencies calculated from identified material parameters match much better to the measured frequencies than calculated frequencies from the material parameters from Ref. [6]; (2) only the first five frequencies are used to identify E_f and G_c, the higher frequencies (from sixth to tenth frequency) can be well predicted.

Table 13
Identified results

	Initial values	Final values	Values in Ref. [6]
E_f (Pa)	9.900e9	9.216e9	9.8e9
G_c (Pa)	5.089e7	4.494e7	3.615e7

Table 14
The measured first 10 frequencies, the calculated frequencies by using the final identified parameters, and their relative errors

Measured frequencies in Ref. [6] (Hz)	Calculated frequencies $E_f = 9.216e9$ Pa $G_c = 4.494e7$ Pa (Hz)	Relative errors with measured frequencies (%)	Calculated frequencies $E_f = 9.8e9$ Pa $G_c = 3.615e7$ Pa (Hz)	Relative errors with measured frequencies (%)
62	62.79	1.2707	64.189	3.530
161	161.02	0.0097	161.532	0.330
288	287.41	0.2045	282.588	1.879
428	427.92	0.0185	413.240	3.449
578	571.72	1.0868	546.822	5.394
726	722.93	0.4222	680.348	6.288
876	871.19	0.5486	812.789	7.216
1026	1018.48	0.7329	943.869	8.005
1172	1144.00	2.3890	1073.654	8.391
1321	1309.38	0.8798	1202.297	8.986

The influence of other initial values on the finally obtained values was also tested. The results are listed in Table 15.

During the different identification processes, only the initial values are different, others such as the convergence criteria remain the same. The identified results are identical by using different initial values.

It can be concluded that: (1) comparing the initial and final identified material parameters in Table 13, it is clear that the proposed procedure for initial value produces good initial values; (2) by changing the initial values (initial values 2 in Table 15), the identified material parameters are identical. The identified procedure is thus stable.

Test case 2: The cantilever beam studied in case 2 in Section 4.1 is also used to verify the proposed identification procedure. The geometric parameters and densities of the cantilever beam are listed in Table 4. The calculated modal frequencies and modal loss factors are used as "virtual experimental values" (VEV). For example, for case $\eta_c = 0.1$, the used VEV calculated by the proposed finite element model are listed in Table 5. The initial values, the identified values and the theoretical values are listed in Table 16. The VEV and the calculated values by using the identified values are listed in Table 17.

Other initial values, for example, E of the face sheets as 7.5e10 Pa, G of the core as 7.5e5 and η loss factor of the core as 0.8, give the same identified parameters.

From the above simulation, it is shown that (1) the loss factors of the core can also be identified from the measured modal loss factors; (2) even a rough approximate initial value can be used to identify the desired material parameters of the sandwich beams with the proposed procedure.

4.3. Error estimation

The sandwich beam with GFRP face sheets and PVC core studied in case 1 in Sections 4.1 and 4.2 is used in this paragraph to validate the error estimation procedure presented in Section 3.

Generally speaking, a typical experimental set-up to measure vibration resonance frequencies includes: (1) an electronic vernier calliper to measure the size of the specimen; (2) an electronic balance to measure the weight; (3) a loud speaker to excite the specimen in an non-contact way;

Table 15
Identified results with different initial values

	Initial values 1	Identified values 1	Initial values 2	Identified values 2
E_f (Pa)	9.9e9	9.216e9	2.46e9	9.216e9
G_c (Pa)	5.1e7	4.494e9	5.56e7	4.494e9

Table 16
The initial values, the identified values and the theoretical values

	Initial values	Identified values	Theoretical values
E of the face sheets (Pa)	6.4e10	6.899999e10	6.9e10
G of the core (Pa)	5.8e5	6.899999e5	6.9e5
η Loss factor of the core	0.13	1.00000e-1	0.1

Table 17
The virtual frequencies, damping loss factors and computed values using the identified material parameters

	No.	VEV	Calculated by using identified values	Relative errors
f_n	1	63.60677073	63.6067695	1.93144E-08
(Hz)	2	294.2024862	294.2024715	5.00096E-08
	3	738.0234346	738.0234074	3.68604E-08
	4	1383.061335	1383.061289	3.29898E-08
	5	2243.210028	2243.209971	2.53116E-08
	6	3316.753505	3316.753421	2.53E-08
η_n	1	2.8131992	2.8131994	6.90588E-08
(%)	2	2.4261244	2.4261247	1.00862E-07
	3	1.544055	1.5440551	1.51117E-08
	4	0.8908146	0.8908145	1.48109E-07
	5	0.5736861	0.5736861	1.09972E-09
	6	0.3908544	0.3908544	8.45715E-08

Table 18
The values and the uncertainty on the input parameters

	Value	Uncertainty interval	Absolute error
f_1 (Hz)	62	61.9–62.1	±0.1
f_2 (Hz)	161	160.9–161.1	±0.1
f_3 (Hz)	288	287.9–288.1	±0.1
f_4 (Hz)	428	427.5–428.5	±0.5
f_5 (Hz)	578	577.5–578.5	±0.5
Length (mm)	1650	1649.99–1650.01	±0.01
Width (mm)	116	115.99–116.01	±0.01
Thickness of GFRP (mm)	2.5	2.49–2.51	±0.01
Thickness of PVC (mm)	50	49.99–50.01	±0.01
Mass of GFRP (g)	0.75603	0.74603–0.76603	±0.01
Mass of PVC (g)	0.96657	0.95657–0.97657	±0.01

(4) a laser vibrometer to pick up signals in an non-contact way; (5) a modal analysis software package; (6) soft cords used to suspend the specimen (to simulate the free–free boundary condition). The values and proposed uncertainties on the input parameters are listed in Table 18.

It can be remarked that the selected error intervals in Table 18 are taken very small. This is only allowed if the test specimen has good homogeneous material properties and if it is machined with proper care. Also, the non-contact excitation and the non-contact measurement on the freely suspended glass beam justify the assumed small error intervals on the measured frequencies. Based on these assumed intervals and the computed sensitivities, it is possible to estimate uncertainty intervals on the obtained material properties by formula (13).

The computed uncertainty intervals for the identified material properties of sandwich beams are listed in Table 19.

According to Eq. (15) in Section 3, the relative contributions of the computed uncertainty of the input parameters are listed in Table 20.

Table 19
The uncertainty interval for the identified material property

	Value	Uncertainty interval	Abs. error	Rel. error (%)
E_f (GPa)	9.216	9.18305–9.24895	0.03295	0.3575
G_c (Mpa)	44.94	44.5045–45.3755	0.4355	0.9691

Table 20
The relative contributions of the uncertainty of the input parameters

	f_1 (%)	f_2 (%)	f_3 (%)	f_4 (%)	f_5 (%)	Length (%)	Width (%)	Thickness of GFRP (%)	Thickness of core (%)	Mass of GFRP (%)	Mass of core (%)
E_f	0.883	1.456	1.001	3.585	46.564	0.355	0.000003	44.147	1.671	0.226	0.113
G_c	0.337	0.518	3.661	46.151	26.250	0.302	0.00002	16.007	6.648	0.085	0.040

From Table 20, the following conclusions can be drawn: (1) the accuracy of the thickness of the face sheets is crucial to the identified Young's modulus; (2) both the thickness of the face sheets and the thickness of the core are important to the identified shear modulus; (3) the higher frequencies play more important roles in the identified results; and (4) the width of the tested sandwich beam has no influence on the final results.

5. Conclusion

In this paper, a finite element model for sandwich beams is developed. An inverse procedure is proposed to identify the material parameters from measured resonance frequencies. It is shown that the Young's modulus of the face sheets, and the elastic shear modulus of the core can be identified by matching the calculated resonance frequencies with the measured resonance frequencies. If the modal loss factors are available, it is also possible to identify the constant loss factor of the core. For free–free sandwich beams with relatively thin, stiff face sheets and relatively thick, soft core, the formulas in Section 2.2 can give good initial values. Compared with a static testing method such as ASTM method [15,16], the proposed method is cheap, convenient and accurate. Furthermore, the proposed inverse method used the complete sandwich beam and is hence non-destructive.

The error estimation results show that the accuracy of the thickness of the face sheets is crucial to the identified Young's modulus, both the thickness of the face sheets and the thickness of the core are important to the identified shear modulus. The higher frequencies play a more important role in the identified results as the lower frequencies.

Acknowledgements

This work was performed in the framework of the inter university research project "GRAMATIC". The research partners are the Katholic University of Leuven and the Free

University of Brussels, both situated in Flanders, Belgium. The project is financially supported by the Flemish Institute IWT for the promotion of Scientific and Technological Research in Industry.

References

[1] F.J. Plantema, *Sandwich construction: The Bending and Buckling of Sandwich Beams, Plates, and Shells*, Wiley, New York, 1966.
[2] H.G. Allen, Z.N. Feng, Classification of structural sandwich panel behaviour, *Proceeding of the EuroMech 360 Colloquium*, Saint-Etienne, France, 1997, pp. 1–12.
[3] P.R. Cunningham, R.G. White, A new measurement technique for the estimation of core shear strain in closed sandwich structures, *Composite Structures* 51 (2001) 319–334.
[4] T. Saito, R.D. Parbery, Parameter identification for aluminium honeycomb sandwich panels based on orthotropic Timoshenko beam theory, *Journal of Sound and Vibration* 208 (2) (1997) 271–287.
[5] E. Nilsson, A.C. Nilsson, Prediction and measurement of some dynamic properties of sandwich structures with honeycomb and foam cores, *Journal of Sound and Vibration* 251 (3) (2002) 409–430.
[6] S. S. Tavalaelly, Wave Propagation in Sandwich Structures, PhD Thesis, Department of Vehicle Engineering, The Marcus Wallenberg Laboratory for Sound and Vibration Research, Stockholm, 2001.
[7] I.M. Daniel, J.L. Abot, Fabrication, testing and analysis of composite sandwich beams, *Composites Science and Technology* 60 (2000) 2455–2463.
[8] A.D. Nashif, D.I.G. Jones, *Vibration Damping*, Wiley, New York, 1985.
[9] C.J. Wiernicki, F. Liem, G.D. Woods, Structural analysis methods for lightweight metallic corrugated core sandwich panels subjected to blast loads, *Naval Engineers Journal* 103 (3) (1991) 192–203.
[10] G. Wang, S. Veeramani, Analysis of sandwich plates with isotropic face plates and a viscoelastic core, *Journal of Vibration and Acoustics* 122 (2000) 305–312.
[11] E.M. Austin, Influences of Higher Order Modelling Techniques on the Analysis of Layered Viscoelastic Damping Treatments, PhD Dissertation, Virginia Polytechnic Institute and State University, Blacksburg, VA, USA, 1998.
[12] G. Wang, Analysis of Sandwich Beams and Plates with Viscoelastic Cores, PhD Dissertation, University of Maryland, USA, 2001.
[13] P. Cupial, J. Niziol, Vibration and damping analysis of a three layered composite plate with a viscoelastic mid-layer, *Journal of Sound and Vibration* 183 (1) (1995) 99–114.
[14] H. Fukuda, G. Itohiya, A. Kataoka, Bending test of CFRP skin/foamed core sandwich plates, *Proceeding of the Sixth Japan International SAMPE Symposium*, Vol. 1, Japan, 1999, pp. 141–144.
[15] ASTM C 273-61, Standard method of shear test in flatwise plane of flat sandwich constructions or sandwich cores (1991).
[16] ASTM C 393-62, Standard method of flexure test of flat sandwich constructions (1991).
[17] T.M. Nordstrand, L.A. Carlsson, Evaluation of transverse shear stiffness of structural core sandwich plates, *Composite Structures* 37 (1997) 145–153.
[18] A. Wanner, K. Kromp, Young' and Shear moduli of laminated carbon/carbon composites by a resonant beam method, in: A.M. Brandt, I.H. Marshall (Eds.), *Brittle Matrix Composites 2*, Elsevier, London, New York, 1988, pp. 280–289.
[19] W. Lins, G. Kaindl, H. Peterlik, K. Kromp, A novel resonant beam technique to determine the elastic moduli in dependence on orientation and temperature up to 2000°, *Review of Scientific Instruments* 70 (1999) 3052–3058.
[20] ASTM, C 1259-01, Standard test method for dynamic Young's modulus, shear modulus, and Poisson's ratio for advanced ceramics by impulse excitation of vibration (2001).
[21] W.P. De Wilde, H. Sol, Coupling of Lagrange interpolation, modal analysis and sensitivity analysis in the determination of anisotropic plate rigidities, *Proceedings of the Forth International Modal Analysis Conference*, Orlando, FL, USA. 1986.
[22] W.P. De Wilde, H. Sol, Determination of the material constants of an anisotropic lamina by free vibration analysis, *Proceedings of the Second International Modal Analysis Conference*, Orlando, FL, USA, 1984.

[23] H. Sol, Identification of Anisotropic Plate Rigidities Using Free Vibration Data, PhD Thesis, Free University of Brussels, 1986.
[24] L.R. Deobald, Determination of Elastic Constants of Orthotropic Plates by a Modal Analysis/Rayleigh–Ritz Technique, Master Thesis, University of Idaho, 1985.
[25] L.R. Deobald, R. F. Gibson, Determination of elastic constants of orthotropic plates by a modal analysis/Rayleigh-Ritz technique, *Proceeding of the Fourth International Modal Analysis Conference*, Los Angeles, FL, USA, 1986.
[26] P.S. Frederiksen, Identification of Material Parameters in Anisotropic Plates, A Combined Numerical/Experimental Method. PhD Thesis, Department of Solid Mechanics, Technical University of Denmark, 1992.
[27] F. Moussu, M. Nivoit, Determination of elastic constants of orthotropic plates by a modal analysis/method of superposition, *Journal of Sound and Vibration* 165 (1993) 149–163.
[28] T.C. Lai, K.H. Ip, Parameter estimation of orthotropic plates by Bayesian sensitivity analysis, *Composite Structures* 34 (1999) 29–42.
[29] H. Hua, Identification of Plate Rigidities of Anisotropic Rectangular Plates, Sandwich Panels and Circular Orthotropic Disks Using Vibration Data, PhD Thesis, Free University of Brussels, Belgium, 1993.
[30] P. S. Frederiksen, Experimental procedure and results for the identification of elastic constants of thick orthotropic plates, Internal Report No. 506, Danish Centre for Applied Mathematics and Mechanics, 1995.
[31] V. Marchand, J.P. Authesserre, Determination of the elastic constants of material, by a free vibration method, *Journal of Sound and Vibration* 194 (1996) 497–512.
[32] M. Grédiac, P.A. Paris, Direct identification of elastic constants of anisotropic plates by modal analysis: theoretical and numerical aspects, *Journal of Sound and Vibration* 195 (1996) 401–415.
[33] W.T. Wang, T.Y. Kam, Determination of elastic constants of composite laminates using measured natural frequencies, *Advance in Composite Materials and Structures* VII (2000) 95–104.
[34] Shun-Fa Hwang, Chao-Shui Chang, Determination of elastic constants of materials by vibration testing, *Composite Structures* 49 (2000) 183–190.
[35] R. Rikards, A. Chate, G. Gailis, Identification of elastic properties of laminates based on experiment design, *International Journal of Solid and Structures* 38 (2001) 5097–5115.
[36] G.R. Liu, K.Y. Lam, X. Han, Determination of elastic constants of anisotropic laminated plates using elastic waves and a progressive neutral network, *Journal of Sound and Vibration* 252 (2002) 239–259.
[37] T.G. Garne, A.R. Martinez, Identification of material constants for a composite structure, *Proceeding of the Ninth International Modal Analysis Conference*, Italy, 1991, pp. 660–670.
[38] Y.M. Shi, The modelling and vibration control of beams with active constrained layer damping, *Journal of Sound and Vibration* 245 (5) (2001) 785–800.
[39] M. Macé, Damping of beam vibrations by means of a thin constrained viscoelastic layer: evaluation of a new theory, *Journal of Sound and Vibration* 172 (5) (1994) 577–591.
[40] A. Fasana, S. Marchesiello, Rayleigh–Ritz analysis of sandwich beams, *Journal of Sound and Vibration* 241 (4) (2001) 643–652.
[41] J.R. Banerjee, Free vibration of sandwich beams using the dynamic stiffness method, *Composite and Structures* 81 (2003) 1915–1922.
[42] V. Birman, C.W. Bert, On the choice of shear correction factor in sandwich structures, *Journal of Sandwich Structures and Materials* 4 (2003) 83–95.
[43] V. Kostopoulos, D.Th. Korontzis, A new method for the determination of viscoelastic properties of composite laminates: a mixed analytical-experimental approach, *Composites Science and Technology* 63 (2003) 1441–1452.
[44] J.C. Lagariasy, J.A. Reedsz, M.H. Wrightx, P.E. Wright, Convergence properties of the Nelder Mead simplex method in low dimensions, *SIAM Journal on Optimization* 9 (1989) 112–147.
[45] M. Hanss, A. Klimke. On the reliability of the influence measure in the transformation method of fuzzy arithmetic, *Fuzzy Sets and Systems* 143 (3) (2004) 277–289.
[46] S.H. Chen, H.D. Lian, X.W. Yang, Interval eigenvalue analysis for structures with interval parameters, *Finite Elements in Analysis and Design* 39 (2003) 419–431.
[47] T. Lauwagie, G. Roebben, H. Sol, W. Heylen, O. Van der Biest, The uncertainty budget of mixed-numerical-experimental-techniques for the identification of elastic material properties from resonance vibrations,

Proceedings of ISMA 2004, *International Conference on Noise and Vibration Engineering*, Leuven, 20–22 September, 2004.

[48] D. Moens, A Non-probabilistic Finite Element Approach for Structural Dynamic Analysis with Uncertainty Parameters. PhD Thesis, Katholieke Universiteit Leuven, 2002.

[49] E.M. Kerwin, Damping of flexural waves by a constrained viscoelastic layer, *Journal of the Acoustical Society of America* 31 (7) (1959) 952–962.

[50] D.J. Mead, S. Markus, The forced vibration of a three-layer damped sandwich beam with arbitrary boundary conditions, *Journal of Sound and Vibration* 10 (1969) 163–175.

[51] C.D. Johnson, D.A. Kienholz, L.C. Rogers, Finite element prediction of damping in structures with constrained viscoelastic layers, *Shock and Vibration Bulletin* 51 (1) (1981) 71–81.

[52] A. Wada, T. Kawasaki, A method to measure shearing modulus of the foamed core for sandwich plates, *Composite Structures* 60 (2003) 385–390.